Biochimica et Biophysica Acta 890 (1987) 179–194
Elsevier

BBA 42069

Photoactivation of the water-oxidizing complex in Photosystem II membranes depleted of Mn and extrinsic proteins. I. Biochemical and kinetic characterization

Noriaki Tamura and George Cheniae

University of Kentucky, Lexington, KY (U.S.A.)

(Received 7 July 1986)

Key words: Water-oxidizing complex; Photoactivation; Manganese; Oxygen evolution

Conditions were defined for obtaining photoligation of Mn^{2+} and photoactivation of O_2 evolution in NH_2OH- and Tris-extracted PS II membranes (TMF-2) completely devoid of the CF_0/CF_1 complex and containing only approx. 2–3 PS II e^- acceptor equivalents per PS II reaction center. At optimal pH (pH 6.5) only light and Mn^{2+} were essential for Mn ligation by the apo-S-state complex (approx. 4 Mn / reaction center); however, Ca^{2+} addition was required for maximal expression of water oxidation activity of the photoligated Mn. In the absence of added PS II e^- acceptors, the quantum efficiency and yield of photoactivation was diminished and was insensitive to atrazine. PS II e^- acceptors increased the quantum efficiency / yield by approx. 2-fold and conferred sensitivity to atrazine. Kinetic analyses of the photoactivation process gave evidence for a rate constraint ($t_{1/2} \approx 125$ ms) and an unstable intermediate (half-life of approx. 1.0 s). Cl^- was not absolutely essential for photoactivation. A 7-fold increase of rate of O_2 evolution was obtained without Cl^- addition to Cl^--depleted NH_2OH-TMF-2; Cl^- addition during photoactivation gave only a 2-fold additional increase. This Cl^- effect ($K_m = 3.8$ mM) was different from the Cl effect ($K_m = 1.5$ mM) on O_2 evolution. Weak light ageing of NH_2OH-TMF-2 in the absence (but not in the presence) of Mn^{2+} inhibited photoactivation and photoreduction of DCIP by Mn^{2+}; however, DCIP photoreduction by DPC or TPB was not diminished. Such weak light ageing also increased the VLP-form of Cyt *b*-559, but there was no apparent correlation between the increase in O_2 evolution and the conversion of the VLP- and LP-Cyt *b*-559 to the HP-Cyt *b*-559 during photoactivation. Photoactivation is suggested to be a two-quantum process in which two Mn^{2+} are sequentially bound, photooxidized and ligated by the apo-S-state complex. This process facilitates ligation of two additional Mn ions to form the tetra-Mn S-state water-oxidizing complex.

Abbreviations: TMF-2, oxygen-evolving Triton X-100-prepared Photosystem II membrane fragment; PS II, Photosystem II; CF_0/CF_1, hydrophobic/hydrophilic components of the coupling factor; apo-S-state complex, the Mn-depleted, inactive water-oxidizing complex of Photosystem II; DCIP/$DCIPH_2$, the oxidized/reduced forms of 2,6-dichlorophenolindophenol; P-680, the reaction center chlorophyll *a* complex of Photosystem II; V_{O_2}, rate of O_2 evolution activity; Chl, chlorophyll; Mes, 4-morpholineethanesulfonic acid; Hepes, 4-(2-hydroxyethyl)-1-piperazineethanesulfonic acid; Tricine, *N*-[2-hydroxy-1,1-bis(hydroxymethyl)ethyl]glycine; TPB, tetraphenylboron; DPC, diphenylcarbazide; DCMU, 3-(3,4-dichlorophenyl)-1,1 dimethylurea; PBQ, phenyl-*p*-benzoquinone; FeCN, potassium ferricyanide; Q_A, Q_B, primary and secondary quinone acceptors of Photosystem II; A_H, high-potential acceptor of Photosystem II; VLP-, LP- and HP-Cyt *b*-559, the very-low-potential, low-potential and high-potential forms of cytochrome *b*-559; Z/Z^+, the reduced/oxidized secondary electron donor of Photosystem II; HQ, hydroquinone; Cyt, cytochrome.

Correspondence: G. Cheniae, N-205, Ag Sci. N, University of Kentucky, Lexington, KY 40546-0091, U.S.A.

Introduction

The water-oxidizing complex of photosynthesis is comprised minimally of 2 (Refs. 1–3) or 4 Mn (see reviews Refs. 4–8), three extrinsic proteins (17, 23 and 33 kDa), Ca^{2+}, and Cl^- in close association with the PS II core complex containing intrinsic proteins (47, 43, 34 and 32 kDa and Cyt *b*-559), quinones, pheophytin, carotenoids and the chlorophyll complexes including P-680 (see reviews Refs. 8–12). A 10 kDa protein also is a part of the multi-component PS II core/water-oxidizing complex, but its function(s) is less clear than perhaps some of the other proteins [13]. The polynuclear Mn-S-state water-oxidizing catalyst [1–3,11,12] is ligated principally with the intrinsic 34 kDa [14–16], secondarily with the extrinsic 33 kDa [16–18], and possibly also with the extrinsic 23 kDa protein [19,20]. The Ca-binding sites in the PS II/S-state complex are associated with proteins other than the 17 and 23 kDa proteins [21–23].

Little is known regarding the mechanism of assembly of these components into or on chloroplast membranes which results in the capacity of the PS II assemblage to carry out the charge-separating and water-oxidizing chemistry. It seems clear, however, that formation/assembly of the catalytically active Mn-S-state water complex is dependent on the photoactivation process [16,24–26]. In this multiquantum process driven by PS II quantum events, Mn^{2+} is incorporated into the assemblage via processes presumably involving oxidation of Mn^{2+} [27,28], a conclusion consistent with identification of valency states of Mn larger than +2 in the S-state complex of chloroplasts/PS II membranes [8,10–12]. This photoligation of Mn^{2+} is accompanied by assembly of the 17 and 23 kDa proteins into the PS II/S-state complex [29,30]. On the other hand, conditions precluding photoligation of Mn^{2+} into the apo-S-state complex increase the susceptibility of the oxidizing side of PS II reaction centers to photoinhibition from which the recovery of PS II trap function and photoactivation is dependent on synthesis of the intrinsic 34 kDa (D_2) polypeptide [31].

Ca^{2+}, in addition to Mn^{2+}, has been recognized to be essential for overall photoactivation and expression of water-oxidizing activity by chloroplasts/PS II membranes devoid of functional S-state centers [16,24–26]. Using intact chloroplasts from leaves grown under intermittent flashes, Ono and Inoue [25] could observe Mn^{2+} and Ca^{2+} competition in the photoactivation process when A23187, an ionophore for divalent cations, was used to confer divalent cation requirements. In the system, a PS-I-reducible stromal factor was required [32]; additionally, the photoactivation of the water-oxidizing complex was accompanied also by an approx. 2-fold increase in the rate of DPC → DCIP photooxidation by PS II [32]. Both these latter results contrast to conclusions reached previously from studies of photoactivation of dark greened algae [33]. Apparently, dissimilar processes, dependent on the system studied, affect the photoactivation mechanism.

In attempts to clarify the roles of Mn^{2+}/Ca^{2+} in photoactivation, any functions of the PS II extrinsic proteins, and the requirements of PS II e^- acceptors, we studied the photoactivation process using PS II membranes depleted of Mn and specific extrinsic proteins. Preliminary data [16] showed that 17, 23 and 33 kDa-less PS II membranes depleted of Mn by $DCIPH_2$-extraction could photoligate Mn and express water-oxidizing activity following dark reconstitution of the membranes with the 33 kDa protein. These data, obtained with PS II membranes having everted orientation [8,10], do not support the postulate [34,35] offered to explain photoactivation observed with various cells [4] and chloroplasts [24,25]. According to Refs. 34 and 35, ligation of Mn^{2+} as a polynuclear complex is a dark process, but PS II quantum events are required to transport Mn^{2+} across the thylakoid (see, however, Refs. 4 and 25).

Here we report conditions and requirements for obtaining ligation of Mn and expression of water oxidizing activity in NH_2OH- and Tris-extracted PS II membranes. Additionally, we show that the kinetics of photoactivation with NH_2OH-extracted PS II membranes are very similar to those obtained with algae and isolated chloroplasts [4].

Methods and Materials

Preparation and extraction of O_2-evolving PS II membranes

PS II membranes (TMF-2) from 7–9 day wheat

seedlings were prepared as described in Refs. 36 and 37. Such membranes ($V_{O_2} \geq 600$ O_2 per mg Chl per h; approx. 4 Mn/200 Chl) have a PS II unit of 200–230 Chl and a PS II electron-acceptor pool size of approx. 2.5 equiv/trap [36,37]. TMF-2 was either used directly or after storage at −80°C. When stored at −80°C, the membranes were washed once (500 μg Chl/ml) in buffer A (0.4 M sucrose/50 mM Mes-NaOH (pH 6.5)/15 mM NaCl) before extraction with NH_2OH or Tris.

NH_2OH-TMF-2 was prepared by extraction of TMF-2 (500 μg Chl/ml) in buffer A with 5 mM NH_2OH for 60 min at 4°C in darkness. The extracted TMF-2 was then pelleted (27000 × *g* for 10 min), washed twice in buffer A (≈ 500 μg Chl/ml), and then resuspended (more than 2 mg Chl/ml) in buffer A. This NH_2OH extraction decreased V_{O_2} and Mn abundance relative to TMF-2 by approx. 98 and approx. 90%, respectively. Equivalent rates and extents of photoactivation were obtained with freshly prepared or −80°C stored NH_2OH-TMF-2. Cl^--depleted NH_2OH-TMF-2 was obtained by washing NH_2OH-TMF-2 in buffer A devoid of NaCl essentially as described in Refs. 36 and 37.

Tris-TMF-2 was prepared similar to NH_2OH-TMF-2 except the extraction (40 min) was made with 0.8 M Tris Cl^-, pH 8.2. The extent of inactivation of V_{O_2} and solubilization of PS II Mn by Tris extraction was comparable to that obtained by NH_2OH. SDS-polyacrylamide gel electrophoresis analyses showed (1) that Tris-TMF-2 was devoid of the 17, 23 and 33 kDa PS II extrinsic proteins, and (2) that NH_2OH-TMF-2 was essentially depled of the 17 and 23 kDa proteins but retained most of the 33 kDa protein.

Photoactivation by continuous illumination or by actinic flashes

Unless otherwise noted, NH_2OH- or Tris-TMF-2 equivalent to 750 μg Chl/ml was preincubated in darkness at 4°C for 15 min in buffer A containing 375 μg 33 kDa protein before photoactivation. Photoactivation routinely was carried out at 23°C in buffer A containing preincubated membranes (250 μg Chl/ml), 1 mM $MnCl_2$ and 50 mM $CaCl_2$. When continuous illumination was supplied, the samples (0.3 ml in 10 ml glass beakers) were illuminated for designated times from above with a fluorescent lamp providing 24 $\mu E \cdot m^{-2} \cdot s^{-1}$ measured at the sample surface. The suspensions were shaken every 5 min. Photoactivation by brief (approx. 2 μs) actinic flashes was done similarly, except for use of a 0.3 cm light path cuvette and a flash lamp arrangement described in Ref. 27.

Following the incubations in light or dark, V_{O2} was determined either directly or following centrifugation (15000 × *g*/10 min) and washing of the membranes at 4°C. Unless otherwise noted, V_{O_2} was determined directly using 20 μl (5 μg Chl) from the incubations. When Mn determinations were to be made, the membranes were pelleted and washed twice (25 μg Chl/ml) in buffer A containing 2 mM EDTA before assay of V_{O_2} and Mn. Such washing diminished V_{O_2} by approx. 20–30% relative to unwashed membranes but removed any adventitiously bound Mn. Atrazine-incubated membranes were washed similarly, except for omission of EDTA in buffer A.

Assay of V_{O_2} and DCIP photoreduction

V_{O_2} was determined polarographically. The assay buffer described in Ref. 20 was used routinely, except where noted when 15 mM $CaCl_2$/33 kDa (10 μg/ml) were included. DCIP photoreduction by Mn^{2+} (50 μM), TPB (50 μM) or DPC (1 mM) was done as described in Ref. 36.

Photosystem II extrinsic proteins

The 17 and 23 kDa proteins were obtained from wheat TMF-2 essentially as described in Ref. 37. The crude protein fraction was either used directly or purified by standard ion-exchange chromatography before use. The 33 kDa protein was obtained by two successive extractions of wheat 17 and 23 kDa depleted TMF-2 (500 μg Chl/ml) with 1 M $CaCl_2$ in buffer A for 1 h at 4°C [16].

Other procedures

SDS-polyacrylamide gel electrophoresis analyses were carried out using a 5% stacking and a 12% polyacrylamide running slab gel. Mn determinations were made by flameless atomic absorption following total digestion of samples and protein determinations were made using bovine serum albumin as the standard [36].

Results

Effects of $MnCl_2$, $CaCl_2$ and 33 kDa extrinsic protein on photoactivation of NH_2OH- or Tris-TMF-2

NH_2OH, Tris and $CaCl_2$/$DCIPH_2$ extraction of PS II membranes causes solubilization of extrinsic PS II proteins ($17 \approx 23 > 33$, $17 \approx 23 \approx 33$ and $17 \approx 23 \approx 33$ kDa, respectively [8–12]) and the tetra-Mn complex. Table I summarizes experiments of the effects of $MnCl_2$, $CaCl_2$ and 33 kDa extrinsic protein on photoligation of Mn and the expression of water-oxidizing activity of photoactivated NH_2OH- and Tris-TMF-2.

Table IA shows the effects of light vs. dark incubation of NH_2OH-TMF-2 on V_{O_2}, determined in the presence and absence of Ca^{2+}, and PS II Mn abundance. Dark incubation under any condition resulted in only small increases of V_{O_2} or PS II Mn abundance. In contrast, light incubation of NH_2OH-TMF-2 in the presence of $MnCl_2$ alone or with $CaCl_2$ (or additionally the 33 kDa) yielded significant increases of V_{O_2} and PS II Mn relative to any of the dark incubated controls. On the other hand, omission of $MnCl_2$ eliminated any light-dependent increase of Mn abundance or V_{O_2} (see Fig. 1A). The light-dependent increase of Mn abundance with Mn^{2+} alone (line 2) proved equal to or greater than the increase observed in the presence of both Mn^{2+} and Ca^{2+} or additionally the 33 kDa protein (lines 3 and 4). However, the V_{O_2} increase of membranes photoactivated in the presence of only $MnCl_2$ was approx. 50% less than those photoactivated in the presence of both

TABLE I

EFFECTS OF $MnCl_2$, $CaCl_2$ AND 33 kDa PROTEIN ON PHOTOACTIVATION OF V_{O_2} AND PHOTOLIGATION OF Mn BY Mn-DEPLETED TMF-2

NH_2OH- or Tris-TMF-2 was preincubated in buffer A in the presence or absence of 33 kDa protein, then photoactivated (40 min at 250 μg Chl/ml) in buffer A containing 100 μM DCIP and, where indicated, 1 mM $MnCl_2$, 50 mM $CaCl_2$ and 125 μg 33 kDa protein (carry over from preincubation). Subsequently, 20 μl (5 μg Chl) of the suspensions were assayed directly. Without photoactivation, the V_{O_2} of NH_2OH- and Tris-TMF-2 was 27.0 and 11.0 μmol O_2 per mg Chl per h, respectively, independent of additions of 2 mM $CaCl_2$ and 33 kDa protein to the assay. Where noted, 15 mM $CaCl_2$ and/or 10 μg 33 kDa protein/ml were added to the assays. Extraction of the variously incubated NH_2OH-TMF-2 with 7.5 mM NH_2OH in buffer A for 20 min diminished their Mn abundance to 0.5 Mn/200 Chl.

A.

NH_2OH-TMF-2	Rate of O_2 evolution (μmol O_2/mg Chl per h)				Manganese abundance (Mn/200 Chl)	
	additions to assay buffer:				dark incubation	light incubation
Additions for photoactivation	dark incubation		light incubation			
	none	$CaCl_2$	none	$CaCl_2$		
1. None	27.8	30.0	31.9	46.0	0.79	0.50
2. $MnCl_2$	24.0	31.3	42.5	197	1.22	3.82
3. $MnCl_2$, $CaCl_2$	19.0	21.3	288	363	0.88	3.33
4. $MnCl_2$, $CaCl_2$, 33 kDa	23.8	32.6	326	346	0.89	3.46

B.

Tris-TMF-2	Rate of O_2 evolution after photoactivation (μmol O_2/mg Chl per h)			
	Additions to assay buffer:			
Additions for photoactivation	none	$CaCl_2$	33 kDa	$CaCl_2$ + 33 kDa
1. None	15.8	16.7	18.5	–
2. $MnCl_2$	22.9	50.3	28.0	–
3. $MnCl_2$, $CaCl_2$	113	152	188	207
4. $MnCl_2$, $CaCl_2$, 33 kDa	186	214	197	–

$MnCl_2$ and $CaCl_2$ when the assay buffer contained 15 mM $CaCl_2$. Other data (to be published elsewhere) show that a fraction of the Mn ligated in the presence of Mn^{2+}, but no Ca^{2+} is bound non-functionally at site(s) other than the apo-S-state complex. With this correction, the good correspondence between increase of V_{O_2} and Mn abundance indicated functional photoligation of Mn^{2+} into the apo-S-state complex. This conclusion was reinforced by observations (text to Table I) indicating that the increased Mn abundance of the photoactivated membranes was susceptible to solubilization by NH_2OH. The requirement of both $MnCl_2$ and $CaCl_2$ for maximum photoactivation of V_{O_2} in NH_2OH-TMF-2 is similar to that reported for $DCIPH_2$-treated $CaCl_2$-TMF-2 [16].

The data of Table IB show the effects of additions of $MnCl_2$, $MnCl_2/CaCl_2$, or $MnCl_2/CaCl_2$/33 kDa protein to the incubation medium and the effects of additions $CaCl_2$, 33 kDa, or $CaCl_2$/33 kDa in the assay of V_{O_2} of Tris-TMF-2 photoactivated at the various conditions. The greater enhancing effect of the 33 kDa protein in the assays of V_{O_2} (with and without 15 mM $CaCl_2$ addition to the assay) of photoactivated Tris-TMF-2 (Table IB) vs. NH_2OH-TMF-2 (Table IA) is consistent with the low abundance of this protein in Tris – relative to NH_2OH-TMF-2. The results obtained with Tris-TMF-2 were in principle similar to those with NH_2OH-TMF-2 and DCIP-treated $CaCl_2$-TMF-2 [16].

The data of Table I for both preparations thus show: (1) only light and Mn^{2+} are essential for the photoligation of Mn^{2+} into the apo-S-state complex of NH_2OH-TMF-2; and (2) Ca^{2+}/33 kDa proteins are not absolutely essential for the photoligation process but are required for maximal expression of water-oxidation activity of the photoactivated Mn-S-state complex.

$MnCl_2$ concentration dependence for photoactivation of V_{O_2}

Fig. 1 shows the dependence of photoactivation on $MnCl_2$ concentrations for NH_2OH-TMF-2 (A) determined in the presence of 5 and 50 mM $CaCl_2$ and for Tris-TMF-2 (B) in the presence of 50 mM $CaCl_2$. In these analyses, the 33 kDa was included routinely in the incubations along with 100 μM

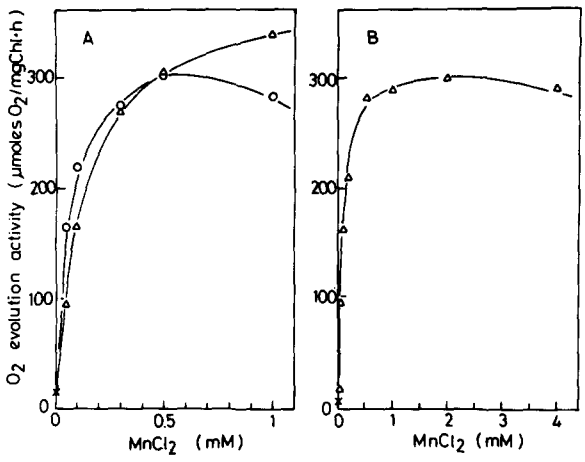

Fig. 1. $MnCl_2$ concentration dependence for photoactivation of V_{O_2} by NH_2OH-TMF-2 (A) and Tris-TMF-2 (B). Photoactivation was done in continuous illumination (see Materials and Methods) in buffer A containing either 5 or 50 mM $CaCl_2$ (circles or triangles, respectively); the $MnCl_2$ concentrations are given on the abscissa. The symbol x denotes V_{O_2} of membranes incubated in darkness with 1 mM $MnCl_2$ and 50 mM $CaCl_2$.

DCIP serving as an electron acceptor. In both cases, photoactivation is strictly dependent on $MnCl_2$ addition. In the presence of 50 mM $CaCl_2$, half-maximal and maximal yield of photoactivation for both Tris- and NH_2OH-TMF-2 were obtained at 100 and 1000 μM $MnCl_2$, respectively (Fig. 1A and B, triangles); however, a decrease in concentration of $CaCl_2$ from 50 to 5 mM (circles) (with NH_2OH-TMF-2) resulted in an approx. 2–2.5-fold decrease of $MnCl_2$ concentration required for both half-maximal and maximal photoactivation. Moreover, the maximal yield of photoactivation was diminished by approx. 11%, and at more than 0.5 mM $MnCl_2$, the yield of photoactivation declined.

Such results agree with those reported for $DCIPH_2$-treated $CaCl_2$-TMF-2 [16]. These $MnCl_2$ concentration values (dependent on $CaCl_2$ concentration) for photoactivation are appreciably greater (approx. 8–10 fold) than those previously reported for photoactivation of Tris extracted chloroplasts, but determined in the presence of only 2 mM Ca^{2+} [38] or for photoactivation of *Anacystis* PS II membranes determined with 54 mM Ca^{2+} [26]. Significantly, the $MnCl_2$ concentration values for photoactivation of NH_2OH-TMF-2 were similar to those required for DCIP

supported photooxidation of Mn^{2+} by NH_2OH-TMF-2 (5 μg Chl/ml). Half-maximal rates of Mn^{2+} photooxidation were obtained at 5 and 80 μM $MnCl_2$, in the absence and presence of 50 mM $CaCl_2$, respectively. The data of Table I and Fig. 1 therefore indicate that the mechanism of photoactivation in NH_2OH-TMF-2 and Tris-TMF-2 membranes is very similar despite significant differences in their polypeptide composition.

Effects of artificial electron acceptors and atrazine

With cells [4] or chloroplasts [24,25], many PS II turnovers are required in the photoactivation process. In contrast to these systems, the PS II acceptor pool in TMF-2 is very limited (approx. 3 equivalents/reaction center [36]). We asked how modification of the acceptor pool size by either addition of PS II e^- acceptors or an inhibitor of the Q_A/Q_B locus affected photoactivation by NH_2OH-TMF-2.

Fig. 2 shows the effect of increasing concentration of DCIP on photoactivation of NH_2OH-TMF-2. About a 2-fold maximal increase and a half-maximal increase in photoactivation was obtained from addition of 100 and 10 μM DCIP, respectively. For [DCIP] > 100 μM, the DCIP-enhanced photoactivation declined sharply until the yield of photoactivation became less than observed in its absence (Fig. 2, inset). The sharp decline may reflect (1) a back reduction by $DCIPH_2$ (or H_2O_2) of Mn^{3+} [39] which otherwise is utilized in the photoactivation of the apo-S-state complex, or (2) simply 'light screening' of Chl by DCIP.

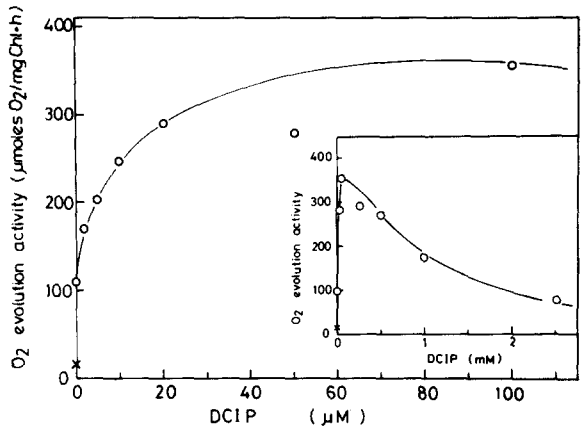

Fig. 2. Effect of concentration of DCIP on yield of photoactivation by NH_2OH-TMF-2 in continuous illumination. The standard protocol for photoactivation was used (see Materials and Methods), except for addition of DCIP concentrations shown. V_{O_2} of the dark incubated control (no DCIP) is shown by the symbol x.

TABLE II

EFFECTS OF ARTIFICIAL e^- ACCEPTORS AND ATRAZINE ON PHOTOACTIVATION OF NH_2OH-TMF-2

Added electron acceptor or inhibitor	Rate of O_2 evolution (μmol O_2 per mg Chl per h)		
	unwashed [a]	washed [b]	inhibition of photoactivation (%)
1. None	173 (1.0) [c]	115	–
2. DCIP (100 μM)	383 (2.21)	257	–
3. FeCN (1 mM)	194 (1.12)	–	–
4. DCIP (100 μM) plus FeCN (1 mM)	138 (0.80)	–	–
5. PBQ (100 μM)	300 (1.73)	–	–
6. PBQ (300 μM) plus FeCN (1 mM)	133 (0.77)	89	–
7. TMPD (100 μM) plus FeCN (50 μM)	253 (1.46)	–	–
8. Atrazine (200 μM)	39	112	3
9. Atrazine (200 μM) + DCIP (100 μM)	38	90	65
10. Atrazine (200 μM) + PBQ (300 μM) + 1 mM FeCN	26	56	37

[a] Following photoactivation for 40 min (Materials and Methods), 20 μl (5 μg Chl) of the suspensions were assayed directly in the 1.0 ml capacity polarographic vessel.

[b] After assay (footnote a), the samples were washed (Materials and Methods) then reassayed. Percent inhibition of photoactivation is based on activity of washed controls.

[c] Numbers in parentheses are relative yields of photoactivation uncorrected for 30.2 μmol O_2 per mg Chl per h of dark-incubated samples.

Data of Table II show: (1) occurrence of photoactivation even in the absence of addition of an electron acceptor; (2) only lipophilic e^- acceptors (DCIP, PBQ, TMPD) give any increase (up to 2-fold) of photoactivation above the level obtained in the absence of an electron acceptor; and (3) addition of FeCN to the lipophilic e^- acceptors inhibits the stimulatory effect of the lipophilic e^- acceptors and, moreover, decreases (approx. 20%) the yield of photoactivation observed in the absence of an added e^- acceptor.

Also shown is the effect of atrazine on photoactivation measured in the absence and presence of added e^- acceptors. Atrazine, like DCMU, reversibly inhibits at the Q_A/Q_B locus [40]. At a concentration (160 atrazine/200 Chl) sufficient to inhibit V_{O_2} virtually completely, the extent of photoactivation obtained in the presence of e^- acceptors was diminished approximately to a level measured without them. With some NH_2OH-TMF-2 preparations, however, near complete inhibition of photoactivation (plus DCIP) was observed.

The results of Table II indicate that Q_B is not absolutely essential in the photoactivation mechanism. They also imply that turnover of the reduced Q_A/Q_B acceptors by added e^- acceptors enhances yields of photoactivation by approx. 2-fold. The observed variable extent of atrazine inhibition of DCIP supported photoactivation may reflect variable extents of perturbation of the Q_A/Q_B locus in the NH_2OH-TMF-2 preparations. In chloroplasts, this locus is known to be perturbed by NH_2OH extraction [41].

pH dependence

Fig. 3 shows the pH dependence of photoactivation of NH_2OH-TMF-2 in different buffer systems. The optimum is pH 6.5 with rather sharp declines on either side of this value. This pH profile is similar to the pH profile for photoactivation of $DCIPH_2$-treated $CaCl_2$-TMF-2 [16] but contrasts to the pH 7.8 optimum reported [32] for Tris-extracted chloroplasts. The observed precipitous decline at pH > 7.0 was more severe when Hepes (Fig. 3, triangles) rather than Tricine (Fig. 3, squares) was employed. Significantly, in measurements of DCIP photoreduction by Mn^{2+} at pH > 7.0 we observe: (1) greater rates of photoreduction in the presence of Tricine than in Hepes; and (2) greater rates of $DCIPH_2$ backreaction (presumably with photogenerated Mn^{3+}) in Hepes than in Tricine following cessation of illumination. These analyses (to be published elsewhere) indicate that the backreaction of $DCIPH_2$ with Mn^{3+} may be a determinant of the sharp decline in DCIP-enhanced photoactivation at pH 6.5. They imply that Mn^{3+} may be required in the photoactivation mechanism [36].

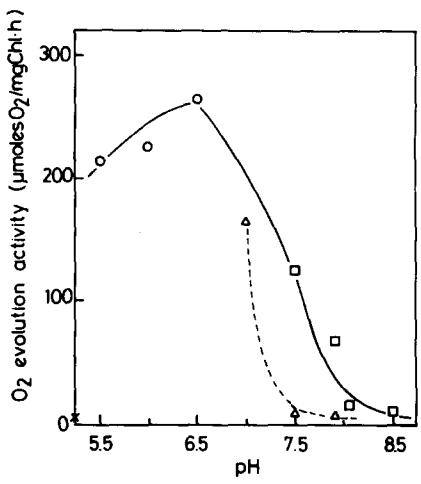

Fig. 3. The effect of pH on photoactivation of V_{O_2} by NH_2OH-TMF-2. NH_2OH-TMF-2 was illuminated (see Materials and Methods) in 0.4 M sucrose/15 mM NaCl/1 mM $MnCl_2$/50 mM $CaCl_2$/100 μM DCIP and 50 mM Mes-NaOH (circles), Tricine-NaOH (squares) and Hepes NaOH (triangles) at the pH values indicated. The symbol x denotes V_{O_2} of membranes incubated in darkness at pH 6.5.

Kinetics of photoactivation of NH_2OH-TMF-2

Fig. 4A shows typical time-courses of photoactivation of NH_2OH-TMF-2 obtained at 23°C at a weak but optimum light intensity in the presence of DCIP (Fig. 4A, circles) and in the absence of an added e^- acceptor (Fig. 4A, open triangles). As shown, the omission of DCIP caused an approx. 50% decrease in photoactivation, which was not affected by atrazine (Fig. 4A, closed triangles). Fig. 4B shows a semilogarithmic plot of the population of the inactive apo-S-state water-oxidizing complex vs. time of illumination of NH_2OH-TMF-2 in the presence of DCIP. (In the analyses, we assumed the observed maximum yield of photoactivation represented 100% conversion of the

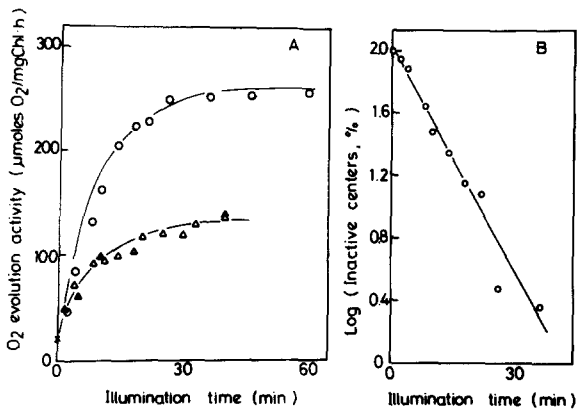

Fig. 4. Time-course of photoactivation by NH_2OH-TMF-2 (A) and a semi-logarithmic plot of the population of the inactive apo-S-state complex vs. illumination time (B). The data of open circles and open triangles were obtained by continuous illumination of NH_2OH-TMF-2 (see Materials and Methods) in the presence and absence of 100 μM DCIP. The closed triangle data were obtained when atrazine (160 atrazine/200 Chl) and no DCIP were used. Atrazine-poisoned samples were washed (see Materials and Methods) before assay of V_{O_2}. Fig. 4B data are the open circle data of Fig. 4A (we assumed the maximum photoactivation was equivalent to complete conversion of the inactive apo-S-state complex to the active S-state complex).

inactive complex to the active water-oxidizing complex.) The resulting straight line implies that the photoactivation of NH_2OH-TMF-2 is a first-order process, a conclusion consistent with that reached with cells [4] or intact chloroplasts [25]; moreover, the observed half-time (approx. 6 min) approximates values reported for the photoactivation of NH_2OH-extracted *Anacystis* ($t_{1/2} \approx 3.2$ min) [42], Tris-treated chloroplasts ($t_{1/2} \approx 7$ min) [24], chloroplasts from intermittent flashed greened leaves ($t_{1/2} \approx 5$–8 min) [32], is greater than reported for the photoactivation of Mn-insufficient *Anacystis* made Mn-sufficient ($t_{1/2} \approx 23$ s) [27], but is less than observed with NH_2OH-extracted leaf segments ($t_{1/2} \approx 1$ h) [31]. The time-courses shown in Fig. 4 were typically observed; however, some NH_2OH-TMF-2 preparations showed a biphasic photoactivation time-course similar to that reported for photoactivation of $DCIPH_2$-treated-$CaCl_2$-TMF-2 [16]. These differing kinetics were observed at either 23°C or 4°C, the latter condition diminishing the rate of DCIP-supported photoactivation by approx. 3-fold. No cogent explanation can be offered for the differing type kinetics.

To analyze the kinetics of photoactivation in more detail, time-courses of flash-induced photoactivation were measured. In the experiments of Fig. 5A, the NH_2OH-TMF-2 membranes were flashed in a train of brief saturating actinic flashes separated by different dark intervals (t_d). At flash spacings of 5 or 10 s, we observed little or no photoactivation; however, with decreasing t_d values the yield of photoactivation increased until

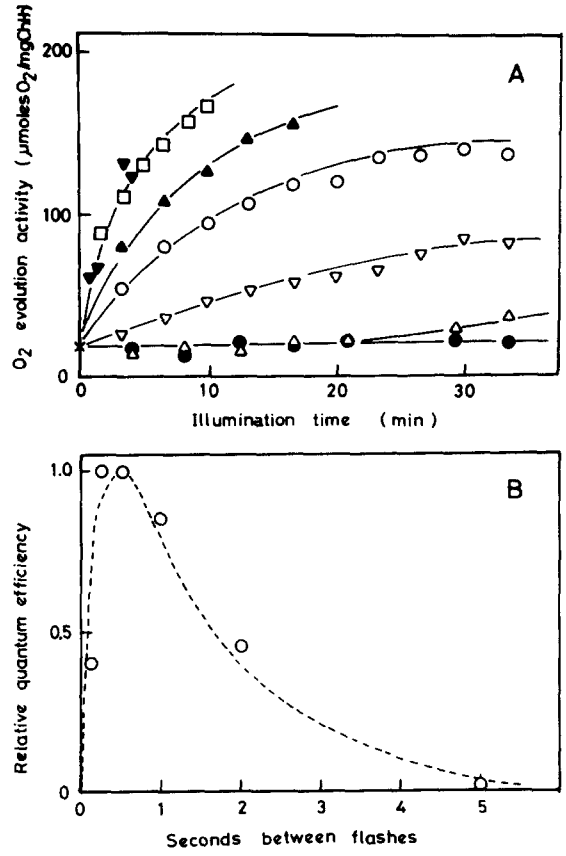

Fig. 5. Analyses of kinetics of dark reactions using brief saturating actinic flashes. (A) NH_2OH-TMF-2 in the standard photoactivation buffer (see Materials and Methods) containing 100 μM DCIP was flash illuminated for times shown. The dark time (t_d) between flashes were: 0.12 s (▼); 0.25 s (□); 0.5 s (▲); 1.0 s (○); 2.0 s (▽); 5.0 s (△); and 10.0 s (●). (B) The initial slopes of curves of Fig. 5A were divided by the total flashes presented within a fixed time interval then the data were normalized to the value obtained with t_d of 0.5 s. The relative values were plotted (open symbols). The dashed line was computed as outlined in Discussion.

ultimately no further increase was observed at $t_d < 0.25$ s. The obtained curves reflect the integrated effect of widely different total numbers of flashes. The initial slopes of the curves divided by the total flashes given within a fixed time interval is a measure of the relative quantum efficiency of the various flash regimes for the conversion of inactive apo-S-state complexes to active water oxidizing Mn-S-state complexes.

In Fig. 5B, we plotted the relative quantum efficiency vs. the time between flashes (t_d) employed in the experiments of Fig. 5A. This analysis shows that the quantum efficiency for photoactivation of NH_2OH-TMF-2 is maximal at t_d of approx. 0.25–0.5 s but declines with either decrease or increase of t_d from this optimal flash spacing. The ascending portion of the curve of Fig. 5B yields an estimate of a rate-limitig reaction ($t_{1/2} \approx 125$ ms) of photoactivation in NH_2OH-TMF-2. The descending portion of the curve reflects the decay ($t_{1/2} \approx 1$–1.5 s) of an unstable intermediate in the overall process of photoactivation of the apo-S-state complex of NH_2OH-TMF-2. Both of these half-times are remarkably similar to the half-times for these proceses determined with cells [27,33,42,43] and chloroplasts [44] lacking functional S-state complexes. Thus, the same kinetic processes deduced previously from in vivo studies of photoactivation of the apo-S-state complex also operate in the photoactivation of NH_2OH-TMF-2.

Anion effects on photoactivation

Fig. 6 and Table III show results of experiments in which we asked if Cl^- was specifically required for photoactivation of Cl^--depleted NH_2OH-TMF-2. These experiments were predicated on arguments that Cl^- serves as a ligand to the Mn ions in the S-state complex [8,9,45] and that Cl^- inhibits the solubilization of Mn from the complex caused by chemical reductants [37]. The results shown were obtained with membranes depleted of Cl^- as described in Methods; However, equivalent results also were observed when sulfate salts of NH_2OH and Na^+ in buffer A were employed for extraction of TMF-2 prior to their washing in Cl^--free buffer A.

In the experiments of Fig. 6A, Cl^--depleted NH_2OH-TMF-2 was photoactivated in the presence of acetate salts of Mn^{2+}/Ca^{2+} and the NaCl concentrations given on the abscissa. In the absence of Cl^- addition, photoactivation yielded an approx. 7-fold increase of V_{O_2} capacity, and an additional 2-fold increase was observed with addition of Cl^-. Fig. 6B shows the Cl^- concentration dependence for expression of V_{O_2} by NH_2OH-TMF-2 photoactivated in the absence of Cl^- (Fig. 6A). These data show an approx. 3.5-fold maximal increase in V_{O_2} by Cl^- added to the assays of photoactivated Cl^--depleted NH_2OH-TMF-2; thus, the membranes used in the experiments of Fig. 6A were significantly depleted of Cl^-. The Cl^- concentration dependence ($K_m = 3.8$ mM) for the increase of photoactivation (Fig. 6A) was appreciably greater than the Cl^- requirement ($K_m = 1.5$ mM) for V_{O_2} of photoactivated Cl^--depleted NH_2OH-TMF-2 (Fig. 6B). These results suggest that Cl^- is not absolutely essential for photoactivation and photoligation of Mn^{2+}; moreover, they suggest any Cl^- effect on photoactivation is different than the Cl^- dependence for the advancement of the S-states in O_2 evolution [8,9].

The data of Table III support the latter conclu-

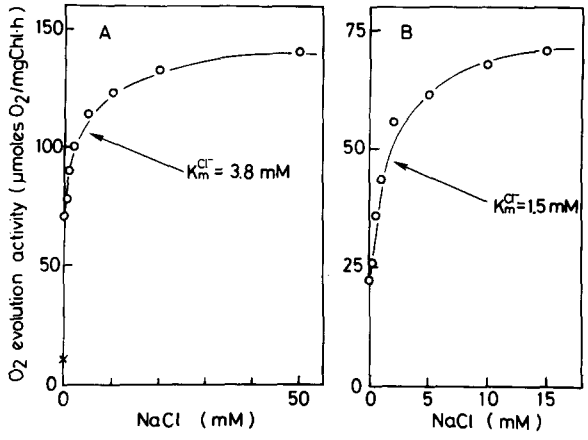

Fig. 6. Cl^- concentration dependence for photoactivation of Cl^--depleted NH_2OH-TMF-2 (A) and for V_{O_2} of NH_2OH-TMF-2 photoactivated in the absence of Cl^- (B). Cl^--depleted NH_2OH-TMF-2 (in the standard photoactivation buffer, except for use of acetate salts of Mn^{2+}/Ca^{2+}) was photoactivated in the presence of the NaCl concentrations shown before assay of V_{O_2} in the standard assay buffer. The symbol x denotes V_{O_2} of dark incubated samples. In (B), V_{O_2} of Cl^--depleted NH_2OH-TMF-2 (photoactivated in the absence of Cl^-) was determined in the presence of the NaCl concentrations shown.

TABLE III

COMPARISON OF THE EFFECTS OF Cl^-, NO_3^- AND SO_4^{2-} ON PHOTOACTIVATION VERSUS EFFECTS ON EXPRESSION OF O_2 EVOLUTION OF PHOTOACTIVATED NH_2OH-TMF-2

Added anion	Rate of O_2 evolution (μmol O_2 per mg Chl per h)	
	Photoactivation [a]	Expression of O_2 evolution [b]
1. None	71 (0) [c]	22 (0)
2. Cl^-	141 (100)	71 (226)
3. NO_3^-	87 (23)	44 (100)
4. SO_4^{2-}	92 (30)	15 (−32)

[a] NH_2OH-TMF-2 (9.6 μmol O_2 per mg Chl per h) was photoactivated for 40 min in the presence of 1 mM Mn acetate and 50 mM Ca acetate and where indicated 50 mM anion as the Na salt. Subsequently, V_{O_2} was determined (Materials and Methods) in the presence of 15 mM NaCl.

[b] NH_2OH-TMF-2 photoactivated in 1 mM Mn acetate and 50 mM Ca acetate were assayed in the absence or presence of Na salts (15 mM anion).

[c] Values in parentheses represent the percent increase or decrease from addition of anion relative to no anion addition.

sion. Either 50 mM NO_3^- or SO_4^{2-} yielded only 20–30% enhancement of the photoactivation obtained in the absence of Cl^-. In contrast, V_{O_2} of photoactivated Cl^--depleted NH_2OH-TMF-2 was enhanced (approx. 100%) by NO_3^-, but inhibited (approx. 32%) by SO_4^{2-}. These differential effects of anions on photoactivation and V_{O_2} of NH_2OH-TMF-2 are qualitatively similar to those reported by Yamashita and Ashizawa [46] for photoactivation of Tris-extracted chloroplasts. They are also qualitatively similar to those for expression of V_{O_2} in Cl^--depleted chloroplasts [9,46,47].

Light- vs. dark-aging effects on photoactivation vs. Photosystem II donor activity

The extent of photoactivation ($\leqslant 70$ μmol O_2 per mg Chl per h) reported [24,34] for Mn-depleted broken chloroplasts is appreciably less than V_{O_2} values (at least 300 μmol O_2 per mg Chl per h) generally reported in the literature for well prepared broken chloroplasts. This difference suggests a significant constraint(s) to the photoactivation process in broken chloroplasts. We asked if possible perturbation of the secondary donor(s) to P-680$^+$ might causally relate to the less than maximum photoactivation.

In the experiments of Fig. 7A, NH_2OH-TMF-2 was preincubated in buffer A at 23°C (Methods) in either weak light (open symbols) or darkness (closed symbols). Following this preincubation, the membranes were photoactivated 40 min in the presence of 100 μM DCIP. As shown, dark preincubation caused minimal loss of photoactivation (approx. 35% after 2 h incubation) compared to weak light preincubation.

Fig. 7B shows results of similar type preincubation experiments in which the effects of preincubation of NH_2OH-TMF-2 in weak light (open symbols) or dark (closed symbols) on the capacity of PS II to photooxidize Mn^{2+} (squares) or DPC (circles) were measured. The results show that dark preincubation affected neither DPC nor Mn^{2+} photooxidation. In contrast, light preincubation diminished Mn^{2+} photooxidation (27 and 40% after 1 and 2 h, respectively), but not DPC (nor NH_2OH nor TPB, data not shown). Such

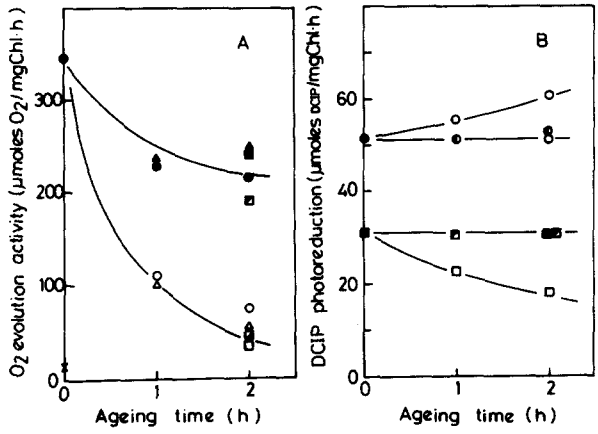

Fig. 7. Effect of ageing of NH_2OH-TMF-2 in weak light and dark on subsequent photoactivation (A) and DCIP photoreduction (B). (A) NH_2OH-TMF-2 was preincubated (see Materials and Methods) at 23°C in buffer A only in either weak light (24 $\mu E \cdot m^{-2} \cdot s^{-1}$; open symbols) or in darkness (closed symbols) for times indicated before addition of $MnCl_2$ and $CaCl_2$ to give 1 and 50 mM, respectively, and subsequent photoactivation for 40 min. The circles and triangles are data from two different experiments. The symbols ◩ and ◪ represent samples aged in light in the presence of 1 mM $MnCl_2$ and 50 mM $CaCl_2$, respectively. (B) NH_2OH-TMF-2 was aged as above in light or dark (open and closed symbols, respectively) in buffer A only before assay of DCIP photoreduction by DPC and Mn^{2+} (upper and lower sets of curves, respectively). The half-closed symbols represent samples aged in light in buffer A containing 1 mM $MnCl_2$.

loss, as well as the loss of photoactivation during light preincubation (Fig. 7A), was essentially eliminated by inclusion of 1 mM $MnCl_2$ during the light preincubations. $CaCl_2$ (50 mM) added to light preincubation did not, however, diminish either loss of photoactivation or loss of Mn^{2+} photooxidation capacity.

These differential effects of light vs. dark aging on photoactivation and Mn^{2+} photooxidation were essentially independent of pH (pH 6.5–8.5). The results (Fig. 7B) suggest that in the absence of Mn^{2+} weak light can modify/inactivate a site of Mn^{2+} photooxidation that is physically or chemically different than the site of photooxidation of other PS II donors [33,34]. Furthermore, a comparison of the data of Fig. 7A vs. 7B suggests a correlative relationship between the loss of Mn^{2+} photooxidation capacity and photoactivation capacity.

Effects of aging and photoactivation on redox properties of cytochrome b-559

Studies of the development of PS II and appearance of V_{O_2} have led some workers to postulate that appearance of V_{O_2} and HP-Cyt *b*-559 are correlated events (Ref. 48; see, however, Ref. 49). This correlation is particularly evident when the temperature sensitive LF-2 mutant of *Scenedesmus* is grown at a temperature precluding vs. permitting functional Mn binding and appearance of V_{O_2} [14]. A hypothesis [50] implicating Mn^{2+} photooxidation by LP/HP-forms ($E_m > 200$ mV) of Cyt *b*-559 in the photoactivation process might have relevance to these correlative events. Accordingly, we measured the effects of dark/light preincubations (Fig. 7) and photoactivation on the redox forms of Cyt *b*-559 of NH_2OH-TMF-2.

The total Cyt *b*-559 abundance (1.2/200 Chl) in wheat PS II membranes (Table IV) is intermediate to values (1–2/200 Chl) reported for spinach PS II [51–54]. The effects of light/dark preincubations and photoactivation of NH_2OH-TMF-2 on the redox forms of Cyt *b*-559 reveal the following: (1) the combined abundance of HP-/LP-forms remain high (78.2%) even after 2 h dark preincubation; (2) light preincubation of NH_2OH-TMF-2 (in the presence or absence of Mn^{2+}) or the photoactivation of dark-preincubated membranes causes an approx. 2-fold increase in the VLP-form at the expense of the HP → LP-forms; and (3) light preincubation in the absence of Mn^{2+} followed by a photoactivation regime caused an additional increase in the VLP- as well as an additional increase of the LP-form relative to samples photoactivated following either preincubation in dark or in light plus Mn^{2+}.

Cramer et al. [17] have proposed that photoactivation involves the oxidation of protein bound Mn^{2+} ($E_m \approx 180$ mV) by LP- and HP-Cyt *b*-559. We disfavor this hypothesis based on the data showing approx. 65% inhibition of photoactivation, but only 22% loss of the HP-/LP-forms of Cyt *b*-559 during a regime of 2 h light preincubation and 40 min photoactivation. If we postulate that the HP- but not the LP-form might participate in photoactivation, then, in a similar comparison as above, the 65% inhibition of photoactivation approximates the observed 56% loss of

TABLE IV

EFFECT OF AGEING OF NH_2OH-TMF-2 IN LIGHT VERSUS DARK AND PHOTOACTIVATION ON THE REDOX PROPERTIES OF CYTOCHROME *b*-559

Incubation conditions [a]		Rate of O_2 evolution		Mol Cyt *b*-559 per 200 Chls		
Preincubation	Photo-activation	(μmol O_2 per mg Chl per h)	total	HP form	LP form	VLP form
1. Dark, 2 h	none	31.9	1.20	0.77	0.17	0.26
2. Light, 2 h	none	25.2	1.22	0.54	0.12	0.56
3. Light plus Mn^{2+}, 2h	none	33.0	1.23	0.61	0.09	0.53
4. Dark, 2 h	40 min	261.0	1.23	0.65	0.07	0.51
5. Light, 2 h	40 min	91.1	1.29	0.30	0.29	0.70
6. Light plus Mn^{2+}, 2 h	40 min	286.0	1.27	0.53	0.19	0.55

[a] The preincubation and photoactivation conditions were equivalent to those employed in experiments of Fig. 7.

HP-Cyt *b*-559. It is clear that Mn^{2+} addition to light-preincubated samples diminishes the extent of loss of HP-Cyt *b*-559 and conserves photoactivation; however, it is not clear that the conservation of HP-Cyt *b*-559 and the photoactivation are directly interrelated. Thus, we suggest that HP-Cyt *b*-559 is not a specific indicator of a functional water-oxidizing complex, but rather may be only an indicator of the general state of the microenvironment of the PS II/water-oxidizing complex.

Discussion

Two hypotheses have been advanced to explain why PS II quantum events are required for ligation of Mn^{2+} by the apo-S-state complex and its conversion into a water oxidizing complex: (1) Mn^{2+} must be photooxidized to Mn^{3+} (or Mn^{4+}) before manganese can be ligated and stabilized as a water-oxidizing tetra-Mn complex [28]; and (2) PS II quantum events are required only for Mn^{2+} transport across thylakoids to the apo-S-state complex, located on or within the inner face of the thylakoid, where subsequently Mn^{2+} is ligated via dark processes to form the water-oxidizing tetra-Mn complex [34,35].

Our studies of the mechanism of photoactivation done with PS II membranes essentially depleted of the tetra-Mn complex and the 17 and 23 kDa (NH_2OH-TMF-2) or the 17, 23 and 33 kDa proteins (Tris- or $DCIPH_2/CaCl_2$-TMF-2) lead us to reject the second hypothesis based on a number of arguments. First, these PS II membranes, having an everted orientation such that the apo-S-state complex is in equilibrium with Mn^{2+}/Ca^{2+} of a bulk solution, still require light for religation of Mn^{2+} and activation of O_2 evolution. Second, these membranes contain maximally only approx. 2–3 PS II e^- acceptor equivalents, are totally depleted of the CF_0/CF_1 complex [36,37], and are highly permeable to H^+ (unpublished results). Thus, these PS II membranes probably lack capacity to transport cations by active transport mechanisms.

The results here and in Ref. 16 indicate minimal requirements for photoligation of Mn as a species having latent capacity for catalytic oxidation of water. They are: (1) a PS II reaction center core complex with a native, non-denatured, intrinsic apo-S-state complex; (2) ligation of Mn^{2+} at specific sites within the apo-S-state complex which is not absolutely dependent on added Ca^{2+} (Table I); and (3) light absorption by open PS II traps. Expression of the latent water-oxidizing activity of the Mn-S-state complex minimally requires the 33 kDa protein and/or Ca^{2+} as shown clearly with photoactivated Tris-TMF-2 lacking the 17, 23 and 33 kDa proteins (Table IB).

The scheme of Fig. 8 attempts to incorporate the biochemical and kinetic data obtained here into a model for photoligation of Mn and photoactivation of O_2 evolution. (For purposes of clarity, we omit showing known PS II charge recombination reactions [8,11] which undoubtedly contribute to the overall low quantum efficiency of photoactivation.) The central kinetic features of the model are: (1) the first quantum absorbed

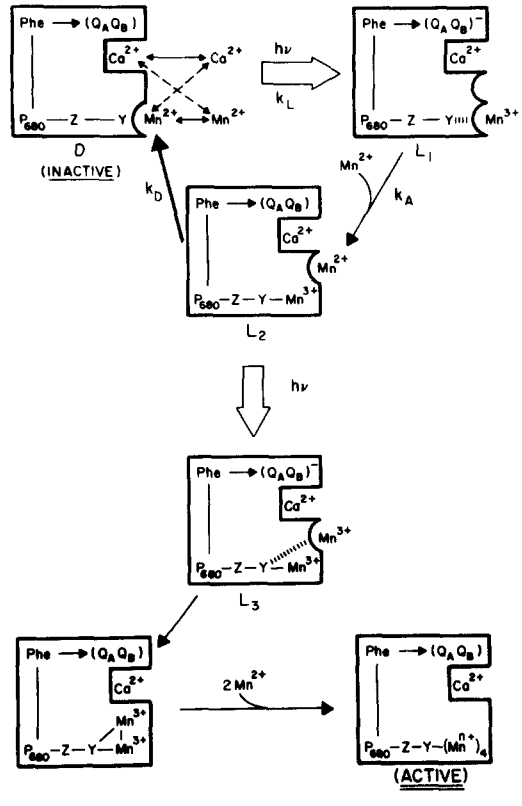

Fig. 8. Model of the mechanism of photoactivation of the apo-S-state water oxidizing complex of PS II. For details, see text.

rapidly converts D * to the unstable intermediate L_1, which is processed to L_2 in darkness by a reaction with rate constant k_A; (2) L_2 is unstable and can decay back to D (k_D) unless processed by a second absorbed quantum to L_3; (3) formation of L_3 results in ligation of Mn as a binuclear complex containing Mn^{3+} which subsequently permits dark ligation of two Mn^{2+} to form the tetra-Mn water oxidizing complex. The latter interpretation may be relevant to those by Satoh and Katoh [56] who showed significant increase of O_2-evolution activity from Mn^{2+} and Ca^{2+} additions to *Synechococcus* PS II membranes containing only 2 Mn/PS II reaction center.

The kinetic model leads to Eqn. 1, which expresses the population of L_2 at t_d after the nth flash:

$$[L_2]_n,\ t_d = \frac{k_A}{k_D - k_A}\phi[D]_{n-1}(e^{-k_A t_d} - e^{-k_D t_d}) \quad (1)$$

where $[D]_{n-1}$ is the population of D after the $(n-1)$th flash and ϕ is the quantum efficiency of the conversion of D to L_2. The photoactivation observed here occurs with very low quantum efficiency ($\phi < 0.01$); however, we cannot determine experimentally whether the inefficiency is a consequence of poor conversion efficiency of D to L_1 or of L_1 to L_2. We therefore rewrite Eqn. 1 into the form of Eqn. 2:

$$[L_2]_n,\ t_d \approx [L_2]_1,\ t_d = \frac{k_A}{k_D - k_A}\phi[D]_0(e^{-k_A t_d} - e^{-k_D t_d}) \quad (2)$$

where $[D]_0$ and $[L_2]_1$, t_d are the population of D and L_2 before and at t_d after the first flash, respectively. We calculated yields of L_2 assuming different values of k_A and k_D then plotted the relative values of L_2 vs. t_d between flashes. The dashed line of Fig. 5B shows results obtained when values used for k_A and k_D were based on half-times of 125 ms and 1.0 s, respectively. A good fit between the predicted and the experimentally observed yields of photoactivation was obtained. This analysis suggests: (1) the conversion of D to L_2 is the limiting step in photoactivation and (2) the photoconversion of L_2 to L_3 occurs rapidly (much less than 125 ms) and with a much higher quantum yield ($\phi \approx 1.0$) than the photoconversion of D to L_2.

The kinetic model describing photoactivation of NH_2OH-TMF-2 is equivalent to the model deduced for photoactivation of *Anacystis* [28]; moreover, the observed/predicted values of k_A and k_D here are very similar to those observed with *Anacystis* [28,42]. However, despite attempts to maximize the quantum efficiency of photoactivation process for NH_2OH-TMF-2, the quantum efficiency proved less than reported for *Anacystis* [27,42], but comparable to that for intermittent light-grown wheat leaves [32] and Tris-extracted chloroplasts [44].

If we accept the two-quantum series model for photoactivation (Refs. 4 and 28; Fig. 8) and the assignment of the approx. 125 ms rate constraint to the conversion of L_1 to the unstable L_2 intermediate, it is not surprising that photoactivation is a slow process even in the presence of added PS II e^- acceptors to maintain Q_A/Q_B in the oxidized forms.

We postulate that the minimal (approx. 2–3-fold) enhancement of photoactivation by PS II e^- acceptors reflects: (1) an increase of the quantum efficiency, a consequence of diminished recombination reactions between reduced Q_A/Q_B and P-680$^+$/Z^+/L_1/L_2; and (2) a decrease of the yield, a consequence of Q_A^- oxidation by the added PS II e^- acceptor(s). The latter postulate is based on the assumption that the species Q_A^--Y^+-Mn^{3+} (L_1 of Fig. 8) must exist for a finite lifetime ($t_{1/2} \approx 125$ ms) in the photoactivation process. This postulate finds some support from the data showing partial (sometimes complete) inhibition of photoactivation by atrazine in the presence of added e^- acceptors (Table III) capable of accepting from Q_A^- [21], but no inhibition by atrazine in the absence of their addition (Table II, Fig. 4A). Apparently, in the latter case, endogenous PS II e^- acceptors such as A_H which is functional in our PS II membranes [29] and the redox forms of Cyt *b*-559 (Table IV) are sufficient to support some of the multi-quantum photoactivation process. Clearly, however, we cannot exclude occur-

* D is comprised of the shown PS II trap components including Cyt *b*-559 (not shown), 1–2 Ca^{2+}/reaction center bound with high affinity (at least 65 μM, unpublished results by K. Cammarata and G. Cheniae) and minimally the intrinsic 34 kDa protein without the tetra-Mn complex.

rence in atrazine poisoned membranes of a low quantum yield processing of $D \rightarrow L_1 \rightarrow L_2 \rightarrow L_3 \rightarrow$ active state, the diminished quantum yield reflecting increased loss reactions arising from increased charge recombination reactions between Q_A^- and the oxidized species of the PS II trap and/or L_1, L_2 and L_3.

We considered a hypothesis [50] invoking a requirement of forms of Cyt *b*-559 ($E_m > 200$ mV) in photoactivation. This hypothesis predicts that the cytochrome would undergo continuous oxidation-reduction cycles during photoactivation, and the rate and/or extent of oxidation by PS II should decrease as active S-state complexes are formed. In chloroplasts, Cyt *b*-559 reduction by the reducing end of PS II is slow ($t_{1/2} \approx 100$ ms) [55], similar to the rate limitation ($k_A \approx 125$ ms) in photoactivation. If, however, Cyt *b*-559 reduction in PS II membranes is similarly slow and oxidation-reduction cycles of Cyt *b*-559 are essential for photoactivation, then added PS II e^- acceptors should have inhibited rather than enhanced the yields of photoactivation (Table II, Fig. 2). The data of Table IV and those in Ref. 49 suggest that HP-Cyt *b*-559 is a poor indicator of functional S-state complexes (see, however, Refs. 14 and 48).

The salient chemical/biochemical points of the photoactivation model shown in Fig. 8 are: (1) a sequential photooxidation by Y^+ * of minimally two Mn^{2+} must occur before their ligation with high affinity by Y; (2) ligation of the first Mn^{3+} (L_1) facilitates the weak binding of the second Mn^{2+} and this occurs via the slow rate-limiting step, k_A, to yield L_2; (3) photooxidation of the second Mn^{2+} yields L_3 which then ligates two additional Mn^{2+} by dark reactions to form a mixed Mn valency state [1–3,11,12], catalytically active tetra-Mn water-oxidizing complex; and (4) Mn^{2+}/Ca^{2+} interactions occur at binding sites for these cations in the PS II complex.

These ideas are predicated on the following observations. First, Mn^{2+} photooxidation, like photoactivation per se but unlike DPC and TPB photooxidation, is diminished by aging of NH_2OH-TMF-2 in light and in the absence of Mn^{2+} (Fig. 7); thus, we believe the Mn^{2+} photooxidation leading to photoactivation must occur by Y^+. Second, steady-state DCIP photoreduction by Mn^{2+} with NH_2OH-TMF-2 shows a slow rate constant ($t_{1/2} \approx 100$ ms) similar to k_A of the photoactivation process. Third, reducing agents such as ascorbate and HQ [33] which serve as PS II donors and/or chemically reduce Mn^{3+} inhibit photoactivation at less than 1 mM concentrations; moreover, with increasing dark time between flashes, the concentration dependence for inhibition decreases [57]. Because equivalent or higher concentrations of ascorbate or HQ do not inactivate V_{O_2} or solubilize the tetra-Mn complex of photoactivated NH_2OH-TMF-2, we conclude the inhibition is a consequence of either competition with Mn^{2+} for Z^+/Y^+ or the reduction of $L_1/L_2/L_3$.

Based on results of Fig. 1A, showing that Mn^{2+} concentrations optimum for photoactivation are affected by Ca^{2+} concentrations, and those of Table IA, indicating that a fraction of the total Mn^{2+} bound during photoactivation can be exchanged/displaced by equilibration with Ca^{2+}, we indicate (Fig. 8) competition between these cations for binding sites within the PS II/apo-S-state complex. This competition between Mn^{2+}/Ca^{2+} may be different than in the model proposed for the photoactivation of A23187-treated intact chloroplasts from intermittent flash grown leaves [25]. In this model, the latent water-oxidation system has two binding sites, each specific for Mn^{2+} and Ca^{2+}, and photoactivation occurs only in centers having both Mn^{2+} and Ca^{2+} on their respective binding sites.

For us to accept the model of Ono and Inoue [25], we must assume that the essential Ca^{2+}-binding site(s) is at least partially occupied in our NH_2OH-TMF-2. This is based on observations showing the photoligation of Mn^{2+} into a significant fraction of the apo-S-state complexes without Ca^{2+} additions (Table IA). We speculate that at least one Ca^{2+}-binding site essential for photoactivation in chloroplasts from intermittent flash-grown leaves reflects the Ca^{2+} requirement for the coupling of PS II traps to the S-state complex [21,23] and Y in Fig. 8. This hypothesis is supported by observations (Cheniae, G., unpublished results) showing that Mn^{2+} is a competitive inhibitor of Ca^{2+} at this site.

* Y^+ is defined as the oxidized species of a PS II donor that is chemically/physically different than Z^+.

Acknowledgements

This work was supported in part by the Department of Energy, Contract DE-AS05-82ER13072. This paper (86-3-140) is published with the approval of the Director of the Kentucky Agricultural Experiment Station. We thank Valery Flynn Thompson for her technical assistance and Iris Deaton for her help in the preparation of the manuscript.

References

1 Wydrzynski, T. and Sauer, K. (1980) Biochim. Biophys. Acta 589, 56–70
2 Dismukes, G.C. and Siderer, Y. (1981) Proc. Natl. Acad. Sci. USA 78, 274–278
3 Kirby, J.A., Robertson, A.S., Smith, J.P., Thompson, A.C., Cooper, S.R. and Klein, M.P. (1981) J. Am. Chem. Soc. 103, 5529–5537
4 Radmer, R. and Cheniae, G.M. (1977) in Primary Processes of Photosynthesis (Barber, J., ed.), Vol. 2, pp. 301–348, Elsevier, Amsterdam
5 Sauer, K. (1980) Acc. Chem. Res. 13, 249–256
6 Cheniae, G.M. (1980) Methods Enzymol. 69, 349–363
7 Amesz, J. (1983) Biochim. Biophys. Acta 726, 1–12
8 Govindjee, Kambara, T. and Coleman, W. (1985) Photochem. Photobiol. 42, 187–210
9 Critchley, C. (1985) Biochim. Biophys. Acta 811, 33–46
10 Ghanotakis, D.F. and Yocum, C.F. (1985) Photosynth. Res. 7, 97–114
11 Van Gorkom, H.J. (1985) Photosynth. Res. 6, 97–112
12 Dismukes, G.C. (1986) Photochem. Photobiol. 43, 99–115
13 Ljungberg, U., Åkerlund, H.E., Larsson, C. and Andersson, B. (1984) Biochim. Biophys. Acta 767, 145–152
14 Metz, J.G., Wong, G. and Bishop, N.I. (1980) FEBS Lett. 114, 61–66
15 Ono, T.-A. and Inoue, Y. (1984) FEBS Lett. 164, 255–260
16 Tamura, N. and Cheniae, G.M. (1986) FEBS Lett. 200, 231–236
17 Ono, T. and Inoue, Y. (1984) FEBS Lett. 166, 381–384
18 Abramowicz, D.A. and Dismukes, G.C. (1984) Biochim. Biophys. Acta 765, 318–328
19 Cammarata, K., Tamura, N., Sayre, R. and Cheniae, G.M. (1984) in Advances in Photosynthesis Research (Sybesma, C., ed.), Vol. 1, pp. 311–320, Martinus Nijhoff/Dr. W. Junk Publishers, Dordrecht
20 Tamura, N. and Cheniae, G. (1985) Biochim. Biophys. Acta 809, 245–259
21 Dekker, J.P., Ghanotakis, D.F., Plijter, J.J., Van Gorkom, H.J. and Babcock, G.T. (1984) Biochim. Biophys. Acta 767, 515–523
22 Boussac, A., Maison-Peteri, B., Vernotte, C. and Etienne, A.-L. (1985) Biochim. Biophys. Acta 808, 225–230
23 Ghanotakis, D.F., Babcock, G.T. and Yocum, C.F. (1984) FEBS Lett. 167, 127–130
24 Yamashita, T. and Tomita, G. (1974) Plant Cell Physiol. 15, 69–82
25 Ono, T. and Inoue, Y. (1983) Biochim. Biophys. Acta 723, 191–201
26 Pistorius, E.K. and Schmid, G.H. (1984) FEBS Lett. 171, 173–178
27 Cheniae, G.M. and Martin, I.F. (1971) Biochim. Biophys. Acta 253, 167–181
28 Radmer, R. and Cheniae, G.M. (1971) Biochim. Biophys. Acta 253, 182–186
29 Becker, D.W., Callahan, F.E. and Cheniae, G.M. (1986) FEBS Lett. 192, 209–214
30 Ono, T.A., Kajikawa, H. and Inoue, Y. (1986) Plant Physiol. 80, 85–90
31 Callahan, F.E. and Cheniae, G.M. (1985) Plant Physiol. 79, 777–786
32 Ono, T. and Inoue, Y. (1982) Plant Physiol. 69, 1418–1422
33 Cheniae, G.M. and Martin, I.F. (1973) Photochem. Photobiol. 17, 441–459
34 Yamashita, T. (1982) Plant Cell Physiol. 23, 833–841
35 Blankenship, R.T., Babcock, G.T. and Sauer, K. (1975) Biochim. Biophys. Acta 387, 165–175
36 Radmer, R., Cammarata, K., Tamura, N., Ollinger, O., and Cheniae, G. (1986) Biochim. Biophys. Acta 850, 21–32
37 Tamura, N., Radmer, R., Lantz, S., Cammarata, K. and Cheniae, G. (1986) Biochim. Biophys. Acta 850, 369–379
38 Yamashita, T. and Tomita, G. (1976) Plant Cell Physiol. 17, 571–582
39 Velthuys, B. (1983) in The Oxygen Evolving System of Photosynthesis (Inoue, Y., Murata, N., Crofts, A.R., Renger, G., Govindjee and Satoh, K., eds.), pp. 83–90, Academic Press Japan, Tokyo
40 Trebst, A. (1980) Methods Enzymol. 69, 675–715
41 Jursinic, P. and Stemler, A. (1983) Plant Physiol. 73, 703–708
42 Cheniae, G.M. and Martin, I.F. (1972) Plant Physiol. 50, 87–94
43 Inoue, Y., Kobayashi, Y., Sakamoto, E. and Shibata, K. (1975) Plant Cell Physiol. 16, 327–336
44 Yamashita, T., Inoue, Y., Kobayashi, Y. and Shibata, K. (1978) Plant Cell Physiol. 19, 895–900
45 Sandusky, P.O. and Yocum, C.F. (1986) Biochim. Biophys. Acta 849, 85–93
46 Yamashita, T. and Ashizawa, A. (1985) Arch. Biochem. Biophys. 238, 549–557
47 Kelly, P.M. and Izawa, S. (1978) Biochim. Biophys. Acta 502, 198–210
48 Cramer, W. and Whitmarsh, J. (1977) Annu. Rev. Plant Physiol. 28, 133–172
49 Ono, T., Nakatani, H.Y., Johnson, E., Arntzen, C.J. and Inoue, Y. (1984) in Advances in Photosynthesis Research (Sybesma, C., ed.), Vol. 1, pp. 383–386, Martinus Nijhoff/Dr. W. Junk Publishers, Dordrecht
50 Cramer, W.A., Theg, S.M. and Widger, W.R. (1987) Photosynth. Res., in the press
51 Sandusky, P.O., Selvius De Roo, C.L., Hicks, D.B., Yocum, C.F., Ghanotakis, D.F. and Babcock, G.T. (1983) in The Oxygen-Evolving System of Photosynthesis (Inoue, Y.,

Crofts, A.R., Govindjee, Murata, N., Renger, G. and Satoh, K., eds.), pp. 189–199, Academic Press Japan, Tokyo
52 Murata, N., Miyao, M., Omata, T., Matsunami, H. and Kuwabara, T. (1984) Biochim. Biophys. Acta 765, 363–369
53 Briantais, J.-M., Vernotte, C., Miyao, M., Murata, N. and Picaud, M. (1985) Biochim. Biophys. Acta 808, 348–351
54 Lam, E., Baltimore, B., Ortiz, W., Chollar, S., Melis, A. and Malkin, R. (1983) Biochim. Biphys. Acta 724, 201–211
55 Whitmarsh, J. and Cramer, W.A. (1977) Biochim. Biophys. Acta 460, 280–289
56 Satoh, K. and Katoh, S. (1985) Biochim. Biophys. Acta 806, 221–229
57 Tamura, N. and Cheniae, G. (1987) in VIIth International Congress on Photosynthesis (Biggins, J., ed.), Martinus Nijhoff, Dordrecht, in the press